Int. J. Electrochem. Sci., 14 **(2019)** 7303 – 7316, doi: 10.20964/2019.08.69

International Journal of
ELECTROCHEMICAL
SCIENCE
www.electrochemsci.org

Corrosion Characteristics of Aluminum in Sodium Bicarbonate Aqueous Solution at 50 °C

Feng Zheng[1], *Liangshou Hao*[1], *Jiayang Li*[1], *Haifeng Zhu*[1], *Xiaoping Chen*[1], *Zheng Shi*[2], *Shengping Wang*[2,*],*Youping Fan*[3,*]

[1] Tianshengqiao Bureau, Extra High Voltage Power Transmission Company, China Southern Power Grid (CSG), Xingyi 562400, China
[2] Faculty of Material Science and Chemistry, China University of Geosciences, Wuhan 430074, China
[3] School of Electrical Engineering, Wuhan University, Wuhan 430072, China
[*]E-mail: spwang@cug.edu.cn (Shengping Wang), ypfan@whu.edu.cn (Youping Fan)

Received: 6 April 2019 / *Accepted:* 12 June 2019 / *Published:* 30 June 2019

This paper considers the corrosion behavior of aluminum in a range of low-concentration sodium bicarbonate solutions at high temperature (50 °C). Aluminum exhibits enhanced corrosion inhibition (passivation) in low concentration sodium bicarbonate solutions when compared to deionized water. It was determined that an aluminum electrode in 1×10^{-3} mol L^{-1} sodium bicarbonate solution (pH 7.77) exhibited the lowest corrosion rate based on the lowest measured corrosion current, the most positive corrosion potential, and the maximum charge transfer impedance. The corrosion of aluminum was inhibited in sodium bicarbonate solution because HCO_3^- anions in the solution developed an ordered charge field at the interface of the aluminum/electrolyte, which limited the diffusion of aluminum ions. This ordered charge fieldmay also enhance the formation of a protective aluminum oxide film, which can effectively inhibit the corrosion of aluminum. The scanning electron microscope (SEM), energy dispersive spectrometer (EDS) and X-ray diffraction (XRD) confirmed that the corrosion products covering the surface of the aluminum electrode were $Al(OH)_3$ and/or Al_2O_3. This paper provides a basis for resolving scaling problems associated with the grading electrode in high-voltage direct current systems caused by the corrosion of the aluminum radiator.

Keywords: Aluminum, Corrosion, Sodium bicarbonate solution, Bicarbonate radical, Radiator, Thyristor, High-voltage direct current

1. INTRODUCTION

High-voltage direct current (HVDC) transmission systems have become the preferred resource allocation and long-distance power transportation method because of their narrow transmission corridor, high transmission efficiency, and low power consumption [1, 2]. The converter valve is the core device

in HVDC and has the function of converting direct current (DC) and alternating current (AC) power [3, 4]. Unfortunately, the scaling problem associated with the grading electrodes in the cooling system of the converter valve can cause many operational disruptions. The aluminum radiator, which is directly in contact with the cyclic inner cooling water, corrodes at high temperatures and high electric fields, resulting in aluminum ions entering the inner cooling water. The aluminum ions move to the surface of the platinum grading electrode through the inner cooling water circulation system, forming deposits due to the electric field and electrochemical effect [5, 6]. Deposits covering the surface of the grading electrode increase the impedance between the grading electrode and water, thus affecting the normal operation of the grading electrode. Furthermore, the deposits will drop into the pipe under the impact of the inner cooling water flow, block the water pipe, and cause breakdown of the device in severe cases. The aluminum in the deposits is derived from corrosion of the aluminum radiator and is precipitated on the surface of the grading electrodes under certain conditions. To resolve the scaling problem of the grading electrode, it is necessary to suppress the corrosion behavior of the aluminum radiator in the inner cooling water system [7]. Previous reports have focused on the corrosion characteristics of aluminum in a weak acid medium (hydrochloric acid, sulfuric acid) [8, 9], aqueous alkaline solutions [10, 11] and neutral dilute salt solutions (for instance, halide media [12, 13] and sodium sulfate solutions [14]).

According to the studies by Weber [15] and Siemen [16], the introduction of a certain concentration of carbon dioxide in deionized water at 25 ℃ can suppress the scaling rate of the grading electrode. Since the scaling on the surface of the grading electrode is a result of aluminum deposition, the studies suggest that the scaling rate was lowered when corrosion of the aluminum radiator in the inner cooling water system was suppressed. It is speculated that HCO_3^- ions play a major role in inhibiting aluminum corrosion when carbon dioxide is introduced into the solution [17]. This paper considers the electrochemical corrosion behavior of aluminum in different concentrations of sodium bicarbonate solution at 50 ℃ with the intent of determining the effect of HCO_3^- ions on aluminum corrosion, which will provide solutions to the scaling problems experienced by grading electrodes in HVDC valve cooling systems.

2. EXPERIMENTAL SECTION

2.1. Electrochemical system

An electrochemical system for testing was composed of a working electrode, a reference electrode, a counter electrode and an electrolyte. Platinum black electrodes were used as the counter electrodes, and the reference electrodes were saturated calomel electrodes (SCEs). The potential of the SCE at 50 ℃ was 0.228 V (relative to the standard hydrogen electrode (SHE)). The working electrodes were cut from the aluminum radiator to provide a 1 cm ×1 cm working surface. The grade of the aluminum electrode was 3003 [18], which is composed of Si (0.57 wt%), Fe (0.63 wt%), Cu (0.14 wt%), Mn (1.27 wt%), Zn (0.09 wt%), Li (0.03 wt%) and Al (97.31 wt%). Apart from the 1 cm^2 working surface, all other surfaces were coated with epoxy resin. Before testing, the working electrodes were

polished with diamond paper and nanoalumina powder, cleaned with deionized water and absolute ethanol, dried and immersed in the testing electrolytes for 24 h.

The electrolytes were deionized water with the following concentrations of sodium bicarbonate: 10×10^{-3}, 5×10^{-3}, 1×10^{-3}, 0.5×10^{-3}, and 0.1×10^{-3} mol L^{-1}. A Mettler Toledo S470 pH meter was used to test the pH of the electrolytes.

2.2. Electrochemical Test

Steady state polarization curves and electrochemical impedance spectroscopy (EIS) spectra were obtained by using a CHI660D electrochemical workstation. The potential scan rate was 1 mV s^{-1} and the potential range was 0.8 V (ranging from a potential of 0.4 V lower than the stable potential to a potential 0.4 V higher than the stable potential). The corrosion potential and corrosion current density were obtained from the polarization curves.

The corrosion characteristics of the aluminum surface were determined from the results of the EIS analysis, which was performed over a frequency range of 1 Hz to 10^5 Hz with an amplitude of 5 mV. The electrolyte temperatures for all tests were between 48-52 °C. The electrochemical system was kept in a shielding box during testing.

2.3. Characterization

All samples for scanning electron microscope (SEM), energy dispersive spectrometer (EDS) and X-ray diffraction (XRD) were subjected to accelerated corrosion by potentiostatic anodic oxidation to observe and analyze the corrosion surface and corrosion products of aluminum more clearly. The anodization process used a two-electrode system with platinum as the cathode and pretreated (polished, washed) aluminum as the anode. The stable potential (open circuit potential) at various concentrations was tested before anodization. Based on the stable potential, the oxidation overpotential of 30 mV was increased to conduct the accelerated corrosion experiments. The corrosion phases were determined using a D8-Focus X-ray powder diffraction instrument with a Cu target. The scanning angle ranged from 5° to 80°, and the scan rate was 8° min^{-1}. SEM was performed using an SU8010 ultrahigh resolution field emission scanning electron microscope equipped with high performance X-ray EDS capabilities.

3. RESULTS AND DISCUSSION

3.1. Polarization curves

The polarization curves of the aluminum electrodes at 50 °C are shown in Fig. 1. The corrosion potential of aluminum in the 1×10^{-3}, 0.5×10^{-3}, and 0.1×10^{-3} mol L^{-1} sodium bicarbonate solutions was higher than that in deionized water, indicating that the corrosion of aluminum in these concentrations of sodium bicarbonate solution was inhibited. However, the corrosion potential of aluminum in the $10\times10^{-}$

^{3} and 5×10^{-3} mol L^{-1} sodium bicarbonate solutions was lower than that in deionized water, indicating that aluminum was more susceptible to corrosion in more concentrated sodium bicarbonate solutions.

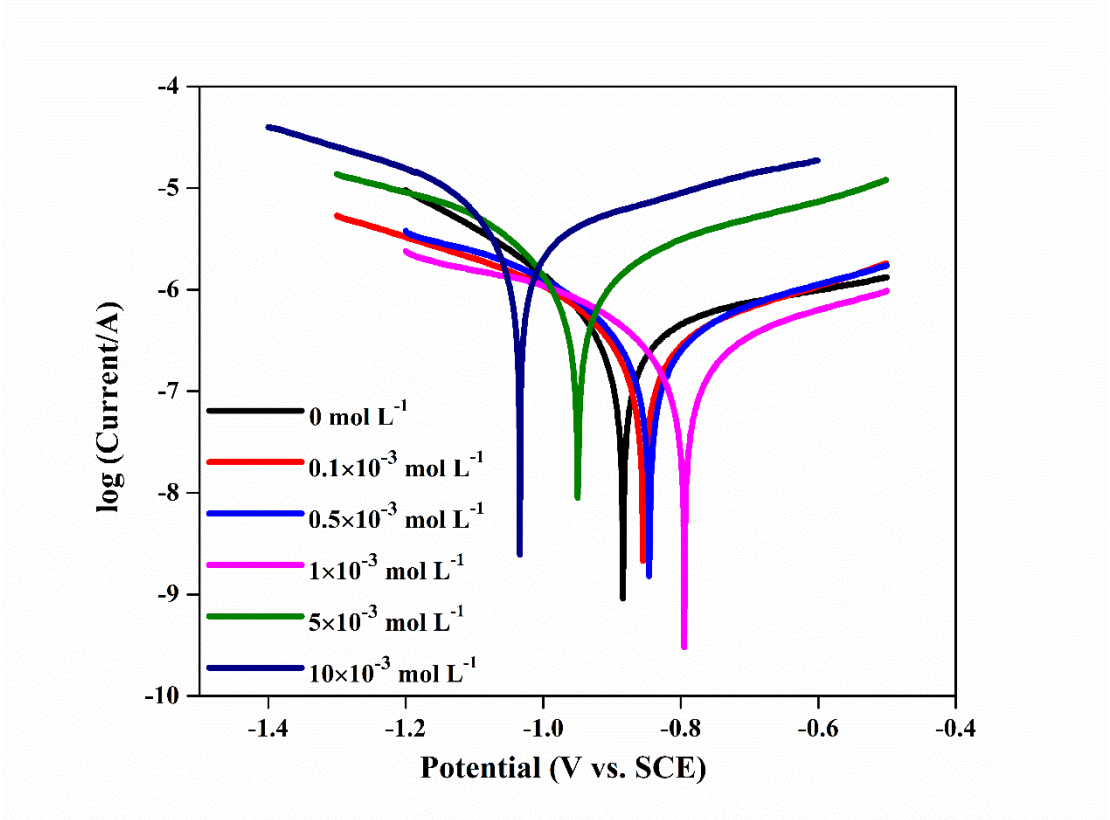

Figure 1. The polarization curves of aluminum in the sodium bicarbonate solutions at 50 °C.

The data for the corrosion potential and the corrosion current density of the aluminum electrodes in the electrolytes are shown in Table 1. The corrosion current of aluminum in the 1×10^{-3}, 0.5×10^{-3}, and 0.1×10^{-3} mol L^{-1} sodium bicarbonate solutions was lower than that in deionized water, but the corrosion current of aluminum in the 10×10^{-3} and 5×10^{-3} mol L^{-1} sodium bicarbonate solutions was higher than that in deionized water.

Table 1. Corrosion potentials and current densities of aluminum in sodium bicarbonate solutions at 50 °C.

Concentration of $NaHCO_3$ ($\times10^{-3}$ mol L^{-1})	Corrosion potential (V)	Corrosion current density ($\times10^{-6}$ A cm^{-2})	Anodic Tafel slope (V dec^{-1})	Cathodic Tafel slope (V dec^{-1})
0	-0.884	5.498	0.209	-0.124
0.1	-0.885	2.561	0.214	-0.161
0.5	-0.846	2.497	0.213	-0.163
1	-0.795	1.905	0.231	-0.184
5	-0.950	9.893	0.193	-0.148
10	-1.034	32.150	0.189	-0.126

The corrosion rate of aluminum in certain concentrations of sodium bicarbonate solutions was lower than that in deionized water. The lowest corrosion current density and the most positive corrosion potential of aluminum were measured in the 1×10^{-3} mol L^{-1} sodium bicarbonate solution, indicating that the corrosion rate of aluminum in this solution was the lowest observed. Therefore, it can be concluded that the corrosion behavior of aluminum in sodium bicarbonate solutions at certain concentrations is inhibited.

3.2. EIS curves

According to the analysis of the surface state of the aluminum electrode, contributions from charge transfer impedance due to oxidation of aluminum, diffusion impedance of ions in the electrolyte, impedance of the electric double layer capacitor, and impedance of the cladding layer should be observed with EIS. The EIS curves of the aluminum electrode in different concentrations of sodium bicarbonate solution are shown in Fig. 2a. The Nyquist diagram of aluminum corrosion in different concentrations of sodium bicarbonate solution indicates similar plots, each consisting of a semicircle and a straight line. The physical meaning of the semicircular diameter in the high frequency region is the charge transfer impedance (Rct) during the corrosion process, which reflects the corrosion resistance of the aluminum in the solution.

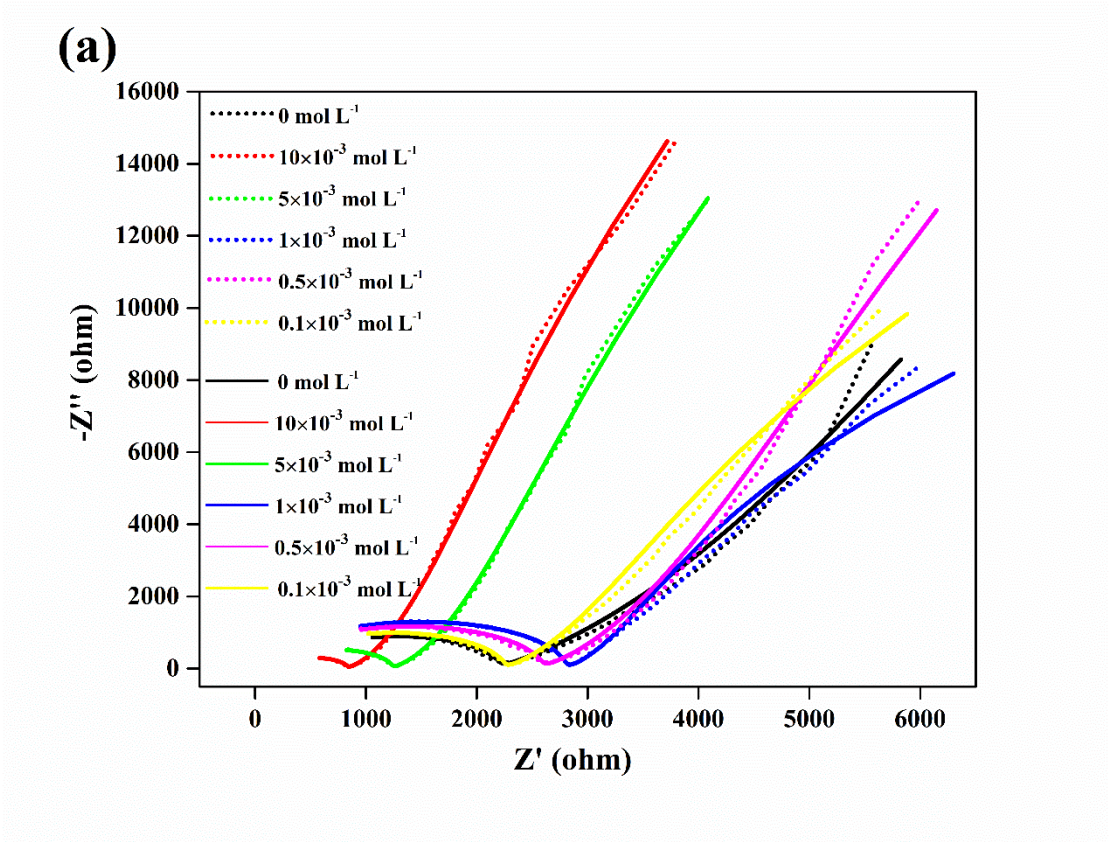

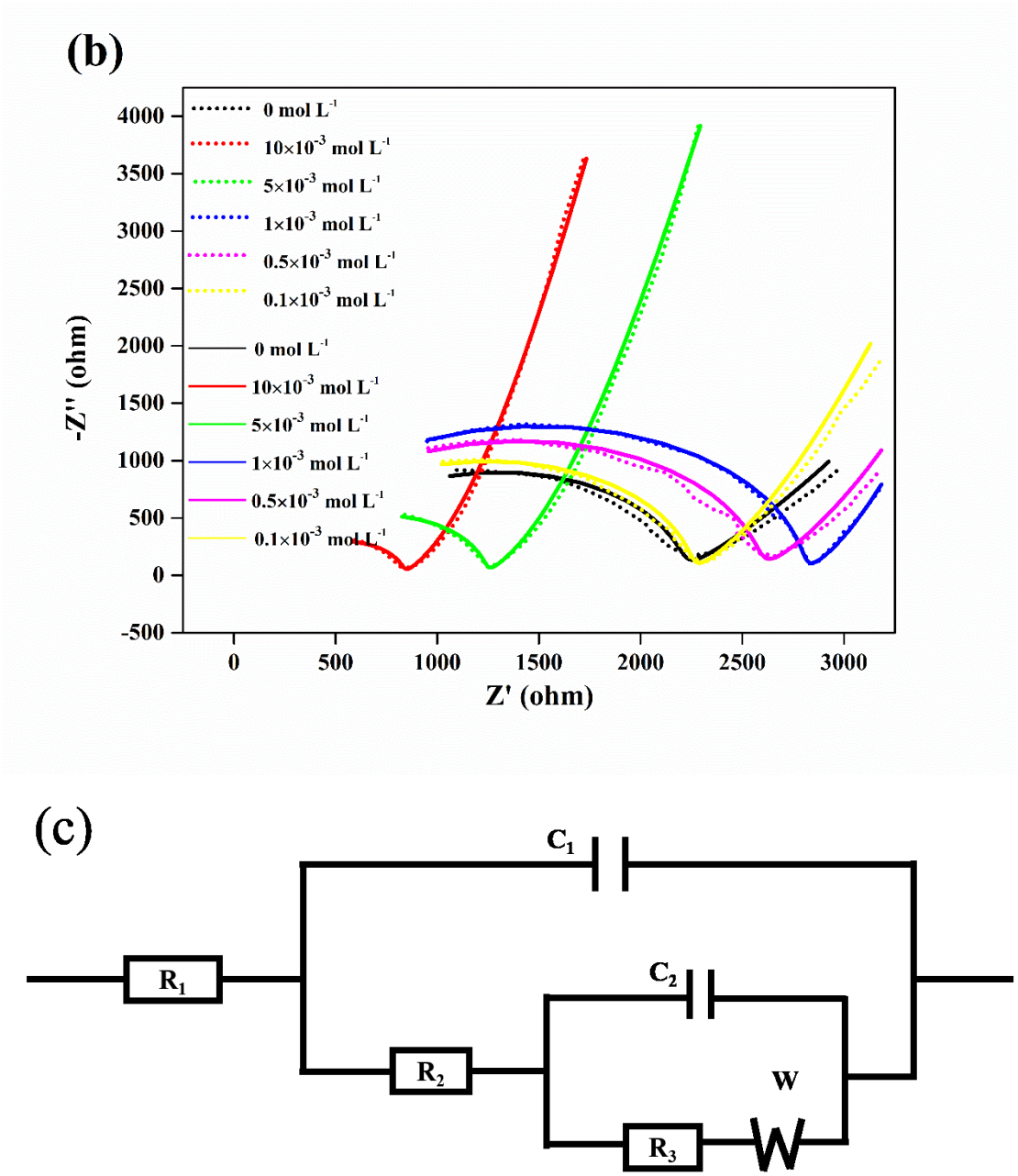

Figure 2. EIS curves (a), partially enlarged EIS curves (b), and the associated equivalent circuit diagram (c) for aluminum electrodes in sodium bicarbonate solution at 50 °C. The original data curves and the fitting curves are indicated by a dotted line and a solid line, respectively.

The equivalent circuit diagram of the electrochemical impedance spectrum is shown in Fig. 2c. R_1 represents the solution resistance between the aluminum electrode and the reference electrode, R_2 represents the impedance of the electrolyte through the deposition layer, R_3 represents the charge transfer impedance for oxidation of aluminum, C_1 represents the capacitance of the cladding layer, C_2 represents the capacitance of the double layer, and W represents the diffusion impedance of ions in the electrolyte [19, 20]. The fitted curves are well matched to the experimental data, which indicates the equivalent circuit diagram is representative of the corrosion reaction of aluminum in the sodium bicarbonate electrolytes.

The data for the corresponding numerical simulation of the equivalent circuit are shown in Table 2. The charge transfer resistance of aluminum in the 10×10^{-3} and 5×10^{-3} mol L^{-1} sodium bicarbonate solutions was lower than that in deionized water, while the charge transfer impedance of aluminum in the 1×10^{-3}, 0.5×10^{-3}, and 0.1×10^{-3} mol L^{-1} sodium bicarbonate solutions was higher than that in deionized water. It was indicated that the corrosion behavior of aluminum in sodium bicarbonate solutions only was inhibited at certain concentrations. The maximum charge transfer impedance was observed in the 1×10^{-3} mol L^{-1} sodium bicarbonate solution, indicating that the corrosion rate of aluminum in the 1×10^{-3} mol L^{-1} sodium bicarbonate solution was the lowest observed. This result is consistent with the polarization curves shown in Fig. 1.

Table 2. EIS parameters obtained by fitting the data to equivalent circuit model.

Concentration of $NaHCO_3$ ($\times10^{-3}$ mol L^{-1})	R_1 (Ω)	R_2 (Ω)	R_3 ($10^{-6}\ \Omega$)	C_1 (10^{-9} F)	C_2 (10^{-6} F)
0	753.0	1773	25.82	1.709	4.346
0.1	396.1	1963	31.49	1.431	7.576
0.5	374.0	235.4	48.35	1.407	6.423
1	273.3	261.5	66.80	1.233	9.418
5	399.8	926.5	9.743	2.335	7.347
10	398.9	509.2	0.543	5.272	6.780

3.3. SEM and EDS

The surface morphologies of the aluminum electrode after corrosion in sodium bicarbonate solution with different concentrations at 50 °C are shown in Fig. 3. Fig 3a shows the presence of significant corrosion on the aluminum electrode surface in deionized water, with gullies, pores and corrosion products observed. Fig. 3e and 3f show that the corrosion of aluminum in the 10×10^{-3} and 5×10^{-3} mol L^{-1} sodium bicarbonate solutions was more substantial and had a rougher surface than that in deionized water. Aluminum was more susceptible to corrosion in more high concentration sodium bicarbonate solutions. However, the corrosion of aluminum in the 1×10^{-3}, 0.5×10^{-3}, and 0.1×10^{-3} mol L^{-1} sodium bicarbonate solutions was mild. The aluminum surface was smooth, with almost no gullies or pores. It was indicated that the corrosion of aluminum in these concentrations of sodium bicarbonate solution was inhibited. It was clearly observed that the aluminum surface was smoothest for the 1×10^{-3} mol L^{-1} sodium bicarbonate solution, indicating that the corrosion rate of aluminum in the 1×10^{-3} mol L^{-1} sodium bicarbonate solution was the lowest.

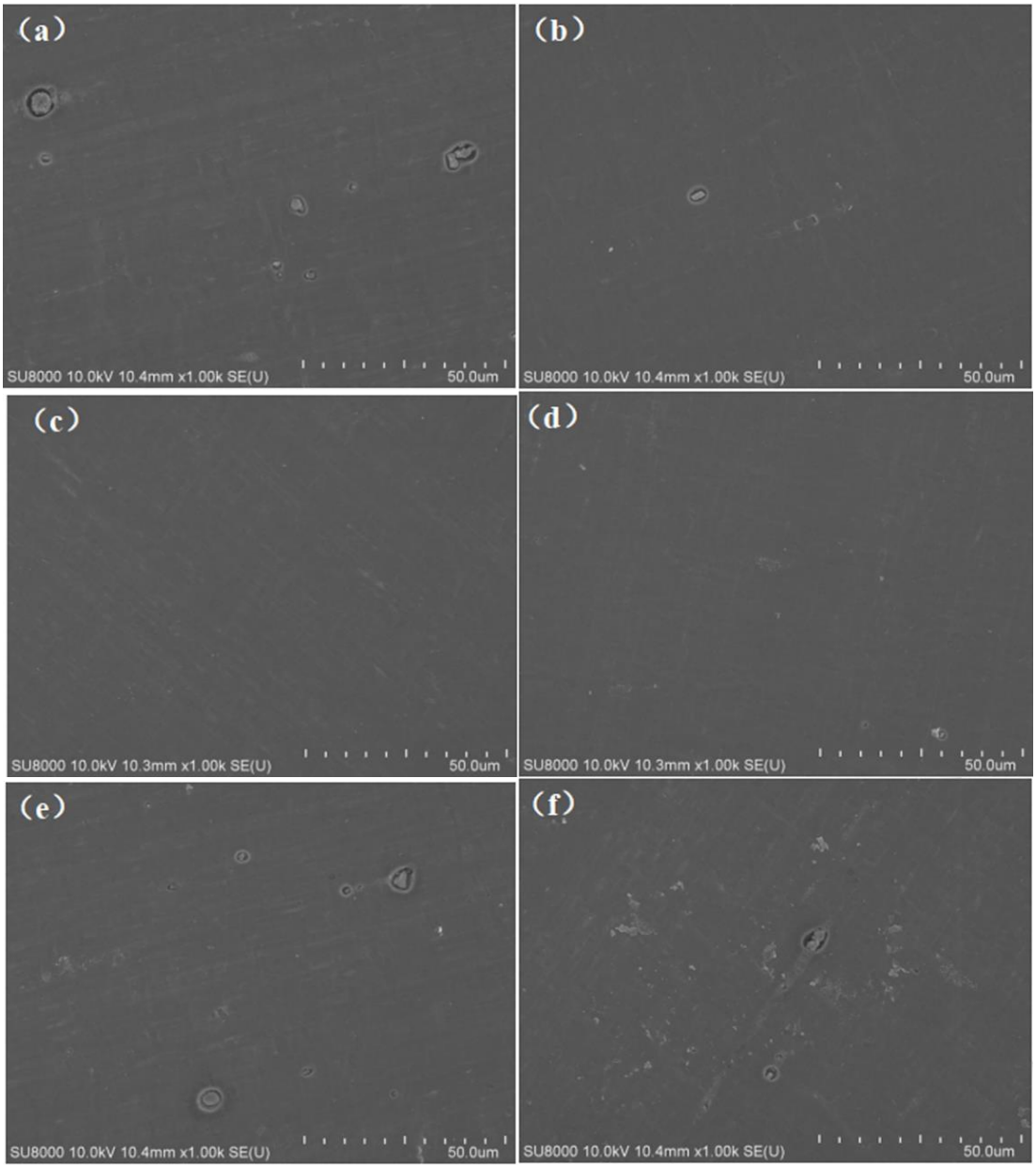

Figure 3. SEM images of the aluminum electrode surface in 0 (a), 0.1×10^{-3} (b), 0.5×10^{-3} (c), 1×10^{-3} (d), 5×10^{-3} (e), and 10×10^{-3} mol L^{-1} (f) sodium bicarbonate solutions.

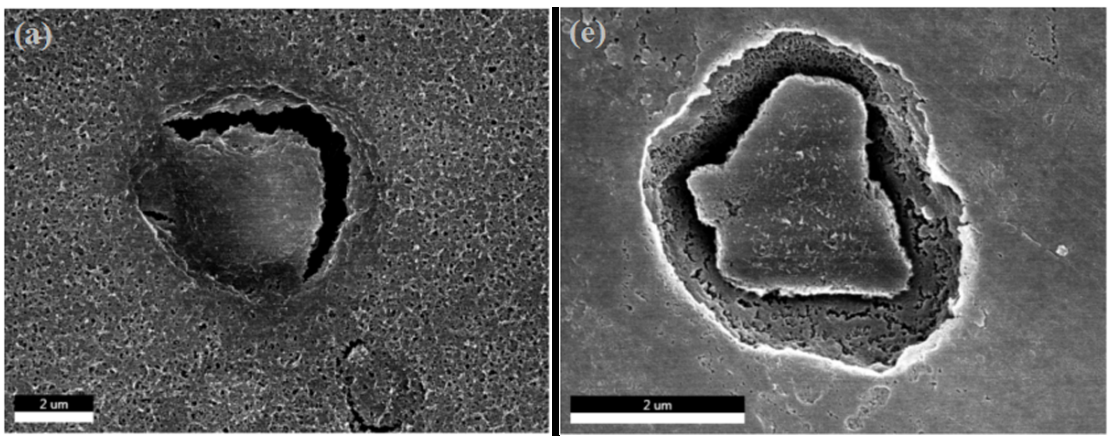

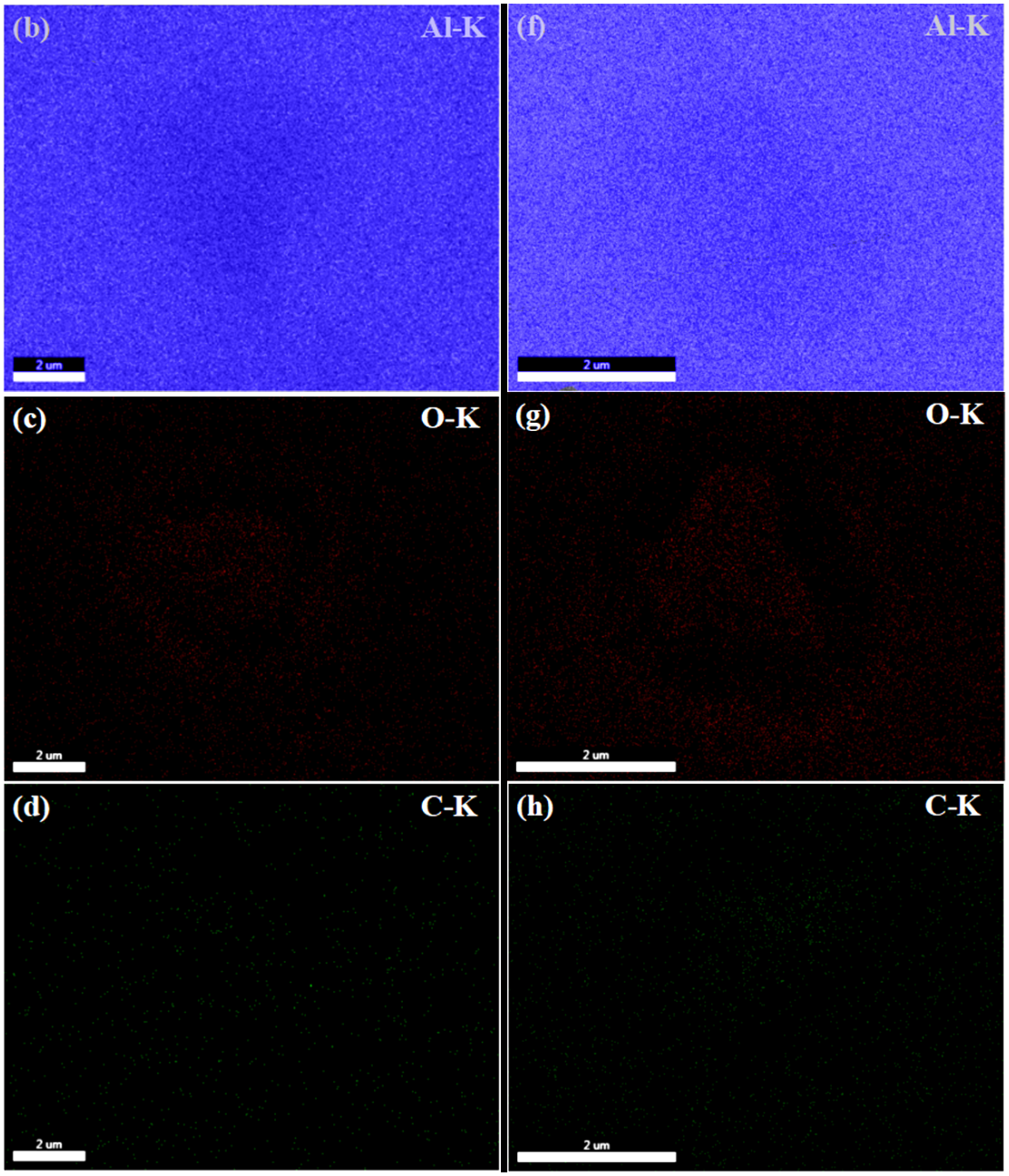

Figure 4. SEM images (a) and Al (b), O (c) and C (d) of EDS elemental analysis for corrosion products of aluminum in deionized water at 50 °C, and SEM images (e) and Al (f), O (g) and C (h) of EDS elemental analysis for corrosion products of aluminum in the 1×10^{-3} mol L^{-1} sodium bicarbonate solution at 50 °C.

The SEM and EDS of the corrosion products of the aluminum electrode in deionized water and the 1×10^{-3} mol L^{-1} sodium bicarbonate solution at 50 °C are shown in Fig. 4. Fig 4a and 4e show that the corrosion of aluminum in deionized water was more severe and there were more pores. According to the EDS elemental diagram for Al and O, the distribution of these elements with respect to the corrosion products in deionized water and the 1×10^{-3} mol L^{-1} sodium bicarbonate solution was similar. Aluminum was uniformly distributed on the electrode surface, while oxygen was mainly concentrated in the corrosion products.

The elemental contents of the corrosion products for the aluminum electrode in deionized water and the 1×10^{-3} mol L^{-1} sodium bicarbonate solution are shown in Table 4. It was found that the elemental composition of the corrosion products were mainly aluminum and oxygen, and there was almost no carbon. The corrosion products of the aluminum electrode in deionized water and sodium bicarbonate solution should be consistent. The corrosion products for the aluminum electrode in the sodium bicarbonate solution did not include either aluminum carbonate or aluminum hydrogen carbonate.

Table 3. The elemental contents from the EDS analysis in Figure 4.

Concentration of $NaHCO_3$ ($\times10^{-3}$ mol L^{-1})	Al-K		C-K		O-K	
	Wt %	*At %*	*Wt %*	*At %*	*Wt %*	*At %*
0	84.51	75.35	12.63	18.90	2.86	5.72
1	84.92	74.61	11.87	18.52	3.21	6.87

3.4. XRD

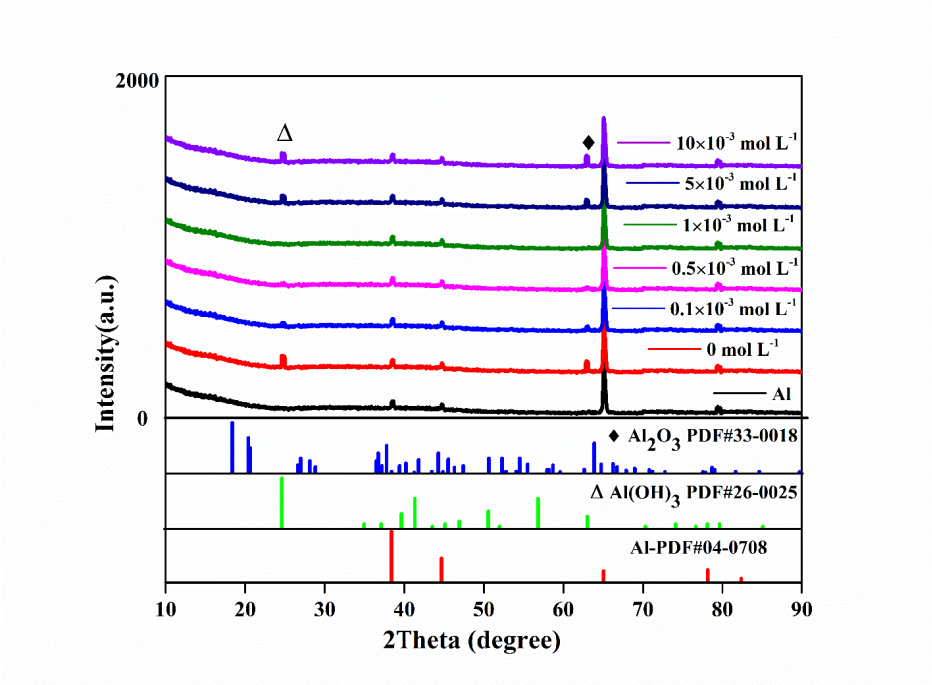

Figure 5. XRD spectra of corrosion products on the aluminum surface in sodium bicarbonate solutions at 50 °C.

The XRD spectra of the corrosion products of the aluminum electrodes in sodium bicarbonate solutions with different concentrations at 50 °C are shown in Fig. 5. For all the samples, four strong peaks are observed at 39°, 45°, 65°, and 78°, these peaks match well to Al (PDF#040-708). Two strong peaks at 25° and 63° also corresponded well to $Al(OH)_3$ (PDF#26-0025) and Al_2O_3 (PDF#33-0018), respectively. This indicates that the corrosion products of aluminum electrodes, in the sodium

bicarbonate solutions and the deionized water, contained $Al(OH)_3$ and Al_2O_3. This is consistent with the corrosion products of aluminum in a moist environment [21, 22]. The peaks at 25° and 63°, for the corrosion products $Al(OH)_3$ and Al_2O_3, were strong for the 10×10^{-3} and 5×10^{-3} mol L^{-1} sodium bicarbonate solutions, while the same peaks were either weak or not discernible for the 1×10^{-3}, 0.5×10^{-3}, and 0.1×10^{-3} mol L^{-1} sodium bicarbonate solutions. Thus, the corrosion of aluminum at certain low concentrations of sodium bicarbonate solution was inhibited.

3.5. Corrosion mechanism

It is speculated that HCO_3^- ions play a major role in inhibiting aluminum corrosion in sodium bicarbonate solutions. As such, the origin of the inhibition of aluminum corrosion by HCO_3^- ions was subsequently investigated.

3.5.1 The effect of pH

A one-step hydrolysis reaction and a second-order ionization reaction of HCO_3^- occur in the sodium bicarbonate solution.

$HCO_3^- + H_2O = H_2CO_3 + OH^-$ (1)

$HCO_3^- = H^+ + CO_3^{2-}$ (2)

$H_2CO_3 = CO_2 + H_2O$ (3)

The equilibrium constants of Formulas (1) and (2) are $K_{a1}=2.1\times10^{-6}$ and $K_{a2}=4.7\times10^{-11}$, respectively. According to reactions (1), (2), and (3) of sodium bicarbonate in water, there are CO_2, H_2CO_3 molecules, HCO_3^-, and CO_3^{2-} ions in the sodium bicarbonate solution. Since there are numerous HCO_3^- ions in the solution, it is speculated that HCO_3^- ions play a major role in inhibiting aluminum corrosion in a carbon dioxide-containing solution.

Pourboix studied the corrosion conditions of various metals and established a potential-pH diagram [23]. During the process of metal corrosion, the potential is the factor controlling the metal ionization process, and the pH is the factor controlling the stability of the metal oxide film. By applying these two factors, many complex homogeneous and heterogeneous chemical reactions between metals and aqueous solutions, and the equilibrium relationship of the electrochemical reactions under given conditions, can be concisely represented on a plane graph. Such graphs visually show the various compounds that metals can produce under different potentials and pH conditions, and the thermodynamic stability of these products. The potential-pH diagram can be used to infer the possibility of metal corrosion and can also inform corrosion prevention strategies by controlling the potential or by changing the pH of the medium.

There are three zones in the potential-pH diagram of aluminum in water, they are corrosion zone, passivation zone and immunity zone. In the immunity zone, the thermodynamically stable form of aluminum is Al, which corrosion will not occur. In the passivation zone, the thermodynamically stable form of aluminum is Al_2O_3, which dense oxide films could be formed on the surface of aluminum to inhibit aluminum corrosion. In the corrosion zone, the thermodynamically stable form of aluminum is

Al^{3+} or AlO_2^-, which the oxide film on the aluminum surface will dissolve such that it cannot protect the aluminum from further corrosion. It is well known that in the range of pH=4~8, aluminum is in the passivation zone [24, 25]. The pH values of 0, 0.1×10^{-3}, 0.5×10^{-3}, 1×10^{-3}, 5×10^{-3} and 10×10^{-3} mol L^{-1} sodium bicarbonate solution at 50 ℃ are 6.12, 6.93, 7.52, 7.77, 8.44 and 8.53, respectively. The pH values for the 10×10^{-3} and 5×10^{-3} mol L^{-1} sodium bicarbonate solutions fall within the corrosion zone, and the pH values for the 1×10^{-3}, 0.5×10^{-3}, and 0.1×10^{-3} mol L^{-1} sodium bicarbonate solutions fall within the passivation zone. Therefore, the corrosion of aluminum in the 10×10^{-3} and 5×10^{-3} mol L^{-1} sodium bicarbonate solutions is substantial, while the corrosion of aluminum in the 1×10^{-3}, 0.5×10^{-3}, and 0.1×10^{-3} mol L^{-1} sodium bicarbonate solutions is mild. After excluding the effect of pH on aluminum corrosion, only the substances in the solution can affect the aluminum corrosion. As the concentration of the sodium bicarbonate solutions gradually increased to 1×10^{-3} mol L^{-1}, the corrosion resistance of aluminum gradually increased. It was the result that HCO_3^- played a major role in inhibiting aluminum corrosion in sodium bicarbonate solutions.

3.5.2 The effect of HCO_3^-

The processes involved in aluminum corrosion phenomena are as follows: damage of oxide/passive film (hydroxylation process) [26, 27], anodic metallic dissolution, and proton reduction [28]. Oxide films are often chemically unstable in aqueous media and dissolve gradually through interaction with water molecules, corresponding to the so-called hydroxylation process. Some specific anions (e.g., Cl^- [29, 30]) at the interface region can facilitate the hydroxylation process at high-energy surface-active sites. However, the HCO_3^- anion is relatively large, is adsorbed at a long distance and brings fewer water molecules onto the surface-active sites. Therefore, HCO_3^- ions inhibit aluminum corrosion by suppressing the dissolution of the oxide film on the aluminum surface.

Aluminum corrosion in sodium bicarbonate solutions is a process of dissolution-precipitation. At the beginning of corrosion, aluminum dissolves and exists in the form of Al^{3+}, aggregating and accumulating on the electrode surface to form a Helmholtz layer. Al^{3+} and OH^- will initially migrate towards each other under the effect of electrostatic attraction, and then react to form insoluble $Al(OH)_3$ deposits. As the deposition process increases, a protective oxide film is formed. As the corrosion process progresses, the aluminum will continue to dissolve into solution to form $Al(OH)_3$. To suppress the corrosion of aluminum, it is necessary to suppress the deposition of aluminum on the surface.

In sodium bicarbonate electrolytes, HCO_3^- was adsorbed on the aluminum surface, eliminating the electric field on the original Al surface. The layer of bicarbonate HCO_3^- became electrostatically repulsive in the sense of charge reversal in the oxide film layer for OH^-, this serves to suppress the deposition of aluminum on the surface. HCO_3^- continuously collected on the surface of the electrode to form a shielding layer, which inhibited the diffusion of aluminum ions into the solution. The Al^{3+} of the Helmholtz layer and aluminum electrodes reached an equilibrium point between dissolution and precipitation. Because the continuous dissolution of aluminum was suppressed, aluminum corrosion was also suppressed.

4. CONCLUSIONS

The corrosion behavior of aluminum in neutral sodium bicarbonate solutions was presented. It was found that aluminum exhibited passivation in low concentrations of sodium bicarbonate solution compared to deionized water, in which corrosion of aluminum was inhibited. In addition, aluminum in a 1×10^{-3} mol L^{-1}, pH=7.77, sodium bicarbonate solution had the lowest corrosion rate, the most positive corrosion potential, and the maximum charge transfer impedance. It was confirmed that HCO_3^- ions played a major role in inhibiting aluminum corrosion in sodium bicarbonate solutions. HCO_3^- inhibited aluminum corrosion by inhibiting the dissolution of the oxide film on the aluminum surface and by the electrostatic repulsion of OH- in solution. This report focused on investigating the primary reason for the corrosion inhibition of aluminum in carbon dioxide-containing solutions. It was determined that HCO_3^- in solution was the key to inhibiting aluminum corrosion and its mechanisms. This paper will provide guidance for the future application of aluminum in HCDC systems.

ACKNOWLEDGMENTS
This work was supported by the Programs of the China Southern Power Grid (CGYKJXM20180405, CGYKJXM20180377).

References

1. A. Kalair, N. Abas, and N. Khan, *Renew. Sust. Energ. Rev.*, 59 (2016) 1653.
2. B.V. Eeckhout, D.V. Hertem, M. Reza, K. Srivastava, and R. Belmans, *Eur. T. Electr. Power*, 20 (2010) 661.
3. N. Flourentzou, V.G. Agelidis, and G.D. Demetriades, *IEEE T. Power. Electr.*, 24 (2009) 592.
4. Y. Jing, Z. Ren, K.J. Ou, and J. Yu, Parameter estimation of regulators in Tian-Guang HVDC transmission system based on PSCAD/EMTDC, *International Conference on Power System Technology*, Kunming, China, 2002, 538-541.
5. H. Qian, Y. Zhou, and C. Xu, *Adv. Mater. Res.*, 354-355 (2012) 1157.
6. Y. Wang, Z. Hao, and R. Lin, *High Vol. Eng.*, 32 (2006) 80.
7. D. Li, Y. Shi, H. Xu, Y. Chen, P. Zhou, X. Li, W. Feng, and S. Wang, *Int. J. Electrochem. Sci.*, 13 (2018) 9346.
8. J.P. Dasquet, D. Caillard, E. Conforto, J.P. Bonino, and R. Bes, *Thin Solid Films*, 371 (2000) 183.
9. I.V. Aoki, M.C. Bernard, S.I.C Torresi, C. Deslouis, H.G. Melo, S. Joiret, and B. Tribollet, *Electrochim. Acta*, 46 (2001) 1871.
10. J. Zhang, M. Klasky, and B.C. Letellier, *J. Nucl. Mater.*, 384 (2009) 175.
11. M. Lashgari, and A.M. Malek, *Electrochim. Acta*, 55 (2010) 5253.
12. B. Zhang, Y. Li, and F. Wang, *Corros. Sci.*, 51 (2009) 268.
13. E. Mccafferty, *Corros. Sci.*, 45 (2003) 1421.
14. S.G. Wang, H.J. Huang, M. Sun, K. Long, and Z.D. Zhang, *J. Phys. Chem. C*, 119 (2015) 9851.
15. I. Weber, B. Mallick, M. Schild, S. Kareth, R. Puchta, and R. Eldik, *Chem. Eur. J.*, 20 (2014) 12091.
16. P.O. Jackson, B. Abrahamsson, D. Gustavsson, and L. Igetoft, *IEEE T. Power Deliver.*, 12 (1997) 1049.
17. D. Li, Z. Shi, H. Xu, Y. Chen, W.X. Feng, Z. Qiu, H. Liu, G. Lv, S. Wang, and Y. Fan, *Int. J. Electrochem. Sci.*, 14 (2019) 3465.
18. C.Y. Kong, R.C. Soar, and P.M. Dickens, *J. Mater. Process Tech.*, 146 (2004) 181.
19. M. Trueba, S.P. Trasatti, and D.O. Flamini, *Corros. Sci.*, 63 (2012) 59.

20. J. Wysocka, S. Krakowiak, J. Ryl, and K. Darowicki, *J. Electroanal. Chem.*,778 (2016) 126.
21. G.S. Frankel, *J. Electrochem. Soc.*, 145 (1998) 2186.
22. R.T. Foley, and T.H. Nguyen, *J. Electrochem. Soc.*, 129 (1982) 464.
23. E. Deltombe, and M. Pourbaix, *Corrosion*, 14 (1958) 16.
24. T. Nishimura, and T. Kodama. *Corros. Sci.*, 45 (2003) 1073.
25. P.A. Brook. *Corros. Sci.*, 12 (1972) 297.
26. M. Lashgari, E. Kianpour, and E. Mohammadi, *J. Mater. Eng. Perform*, 22 (2013) 3620.
27. P.J. Eng, T.P. Trainor, G.E.Brown, G.A. Waychunas, M. Newville, S.R. Sutton, and M.L. Rivers, *Science*, 288 (2000) 1029.
28. E.J. Lee, and S.I. Pyun, *Corros. Sci.*, 37 (1995) 157.
29. M. Lashgari, *Electrochim. Acta*, 56 (2011) 3322.
30. W.M. Carroll, M. Murphy, and C.B. Berslin, *Corros. Sci.*, 34 (1993) 1495.